Available online at www.sciencedirect.com
ScienceDirect
Ceramics International 34 (2008) 1741–1746
CERAMICS INTERNATIONAL
www.elsevier.com/locate/ceramint

A polymer complex solution process for the synthesis and characterization of Ni–YSZ cermet material

Tanja Razpotnik *, Marjan Marinšek, Barbara Novosel,
Klementina Zupan, Vojmir Francetič, Jadran Maček

Faculty of Chemistry and Chemical Technology, University of Ljubljana, Aškerčeva 5, 1000 Ljubljana, Slovenia

Received 24 April 2007; received in revised form 7 May 2007; accepted 20 May 2007

Abstract

Ni–YSZ cermets for SOFC anodes were prepared by the Pechini-type reaction route. The initial polymer precursors were prepared with different citric acid/ethylene glycol (CA/EG) molar ratios. The properties of the samples at different stages of the preparation procedure were evaluated with regard to thermal decomposition (TG–DTA), crystallite size (XRD), surface area (BET), sinterability and phase distribution (SEM). The results showed that an increase of CA and EG in the starting solution increased the final temperature of the thermal decomposition of gels from 340 °C to 382 °C, and the specific surface area of calcined NiO–YSZ powders from 10 $m^2 g^{-1}$ to 27 $m^2 g^{-1}$. In parallel the sinterability of the samples increased. A distinct increase of CA in the predominantly aqueous solution diminished the nickel grain size in the final Ni–YSZ material. A shift from aqueous to organic media further reduced the nickel-rich regions to around 0.2 μm.

Keywords: B. Microstructure-final; E. fuel cells; Ni–YSZ; Sol–gel processing

1. Introduction

High temperature solid oxide fuel cells (SOFC) are electrochemical energy conversion devices in which the chemically stored energy of fuels (hydrogen, methane, methanol, etc.) is directly converted into electrical energy [1,2]. Numerous materials were suggested and tested for SOFC applications and among them the most frequently mentioned are (a) Ni–YSZ cermet as the anode; (b) an ionic conductor of 8 mol% Y_2O_3-stabilised ZrO_2 (YSZ) as the electrolyte; and (c) a perovskite material based on doped $LaMnO_3$ (normally strontium-doped, LSM) as the cathode [1]. The performance of Ni–YSZ cermet is critically dependent on its microstructure, especially the distribution of Ni and YSZ constituents. The anode cermets are usually prepared by mechanically mixing and homogenizing pre-prepared nickel oxide (NiO with a main grain size around 1 μm) and YSZ powders normally bimodally composed of coarser (∼25 μm) and finer (∼0.5 μm) fractions [2]. Such mixtures are subsequently sintered and nickel oxide then reduced to nickel. However, due to mechanical mixing the final composite contain a nonuniform distribution of both components in the anode cermet.

Over the recent years a number of solution-based synthesis routes have been developed and used for the production of ceramic composite materials; co-precipitation methods, the sol–gel processes, oxidation–reduction reactions and hydrothermal syntheses [3]. These methods represent so-called ‘‘soft chemistry’’ which uses relatively nonaggressive diluted solutions at moderate temperatures. The polymerizable complex solution method, i.e. the Pechini method [4] can also be included in this group. One of the main advantages of this process is the possibility of preparing very fine mixtures. Normally, reactive polymerizable complexes are prepared from completely dissolved precursors. This organo-metallic complex formulation enables precursor mixing at the molecular level. Laberty-Robert et al. used this method for the preparation of 8 mol% YSZ [5,6]. Duran et al. [7] and Sun-Dong Kim et al. [8] used the same method for the successful preparation of Ni–YSZ material.

In the present study Ni–YSZ anode materials were prepared by a modified Pechini-type reaction route. The difference from the work already described in the literature [5–8] was that

---

* Corresponding author. Tel.: +386 1 2419 214; fax: +386 1 2419 220.
E-mail address: tanja.razpotnik@fkkt.uni-lj.si (T. Razpotnik).

0272-8842/$34.00 © 2007 Elsevier Ltd and Techna Group S.r.l. All rights reserved.
doi:10.1016/j.ceramint.2007.05.006

starting components were prepared as metal-nitrate aqueous solutions. Hence the cations used for the final cermet preparation were randomly mixed at the beginning of the process. The main objective of this work was to prepare homogeneous and morphologically suitable materials for SOFC application, and to evaluate the influence of some synthesis variables, including the change from predominately aqueous to organic reaction media and alteration of the amount of citric acid, on the final phase distribution in the Ni–YSZ anode cermet.

2. Experimental procedure

NiO–YSZ powders were prepared by the polymerised complex method (PC method), based on the modified Pechini-type reaction route. Subsequent temperature programmed reduction of nickel oxide to nickel produced Ni–YSZ material composed of 8 mol% yttria stabilized zirconia (YSZ) with a nickel content of 50% by volume of the total solid.

Zirconyl nitrate ($ZrO(NO_3)_2 \cdot xH_2O$, Acros Organics), yttrium oxide (Y_2O_3, Aldrich), nickel nitrate ($Ni(NO_3)_2 \cdot 6H_2O$, $6H_2O$, Acros Organics), ethylene glycol ($C_2H_6O_2$, Kemika Zagreb) and citric acid ($C_6H_8O_7 \cdot H_2O$, Carlo Erba) were used for the synthesis as shown schematically in Fig. 1. Denotations of samples in Fig. 1 $[CA]:[EG]:[M] = X:Y:1$ refer to molar ratios between citric acid (CA), ethylene glycol (EG) and total metal ions ($M = n(Ni^{+2}) + n(Zr^{+4}) + n(Y^{+3})$), respectively. The EG/M ratio was maintained the same throughout samples A–D. Sample E was prepared with the same CA/M ratio as sample D but with much higher addition of EG in the starting solution.

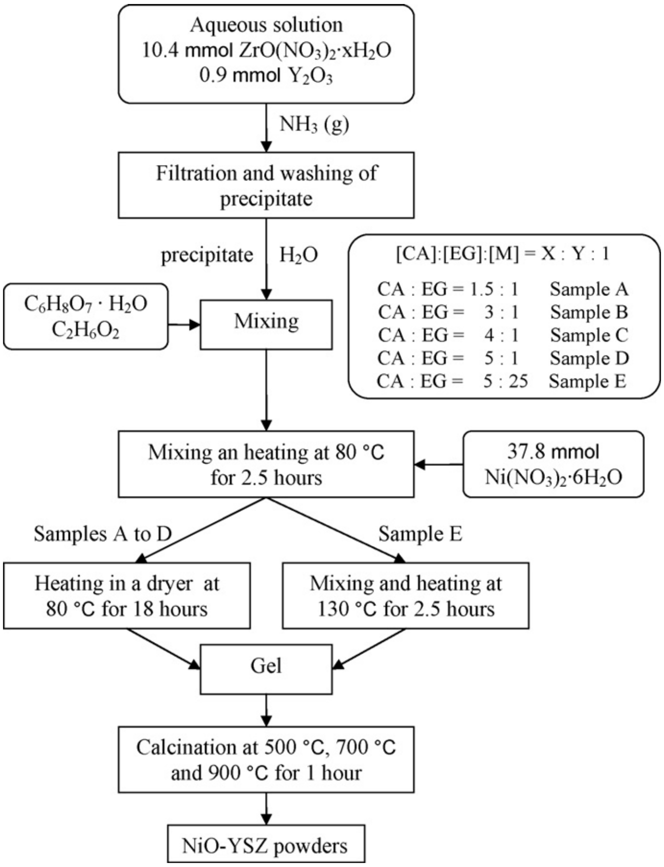

Fig. 1. Flow chart of NiO–YSZ powder preparation with different CA/EG ratios.

Prior to the preparation of samples A–E the Y_2O_3 powder was dissolved in an acidic solution of $ZrO(NO_3)_2$. The pH value of the 0.024 M aqueous solution of zirconium and yttrium precursor was then raised to 9.0 by bubbling gaseous ammonia through it. The precipitate was filtered and washed with distilled water and then transferred to a 1000 mL beaker where it was mixed with 150 mL of distilled water. CA and EG at different CA/EG ratios were also added. During continuous stirring the solution was heated to 80 °C and kept at this temperature for 2.5 h. $Ni(NO_3)_2 \cdot 6H_2O$ was added after the solution had become transparent. For samples A–D solvent evaporation and polyesterification continued without stirring in the dryer for 18 h. The bright green hygroscopic solids obtained were subsequently calcined at 400 °C for 1 h. In the case of sample E the same preparation procedure was used, with the exception that the temperature of the solution increased to 130 °C due to evaporation of water and the higher boiling point of the residual organic medium. Because of this effect, we designated sample E as a sample prepared from organic reaction medium. The solution was kept at this temperature for another 2.5 h. The transparent green gel obtained was immediately calcined at 400 °C for 1 h. All five samples resulted in black powders which were subsequently calcined at 500 °C, 700 °C or 900 °C for 1 h.

The thermal properties of thus prepared gels were determined by thermogravimetry and differential thermal analysis (TG–DTA, Netzsch STA 409) in air with a heating rate of 0.5 °C min^{-1}. The calcined samples were characterized by X-ray powder diffraction using a Brukers D4 Endover instrument employing Cu Kα radiation ($\lambda = 1.5406$ Å). The powder crystallite sizes of samples calcined at 900 °C for 1 h were determined by X-PAS software using the Scherrer equation [10] and X-ray diffraction broadening of different peaks. Specific surface areas of calcined powders were determined after drying the samples for 2 h at 145 °C by the one point BET method (Flow Sorb II 2300, Micromeritics), using nitrogen as an absorbate.

Powders calcined at 900 °C for 1 h were used for the sintering experiments. The samples were homogenised for 30 min in a planetary ball mill (Pulverisette 5, Fritsch) and uniaxially pressed into pellets of 6 mm diameter. By applying appropriate pressures the green density of the tablets was adjusted to 42.2 ± 0.2% of the theoretical value of 6.488 g cm^{-3}. The sinterability of different samples was determined by heating and annealing the pellets in a tube furnace at various temperatures, e.g. 1250 °C, 1300 °C, 1350 °C and 1400 °C, for 1 h. The sintered tablets were polished and afterwards NiO was reduced to Ni in argon ($\varphi = 0.95$)–hydrogen ($\varphi = 0.05$) atmosphere at 900 °C for 2 h. The densities of tablets were calculated as geometrical densities by measuring the mass and dimensions of green, sintered and reduced pellets. The microstructural features of Ni–YSZ composites were determined by scanning electron microscopy (Zeiss FE SUPRA 35 VP).

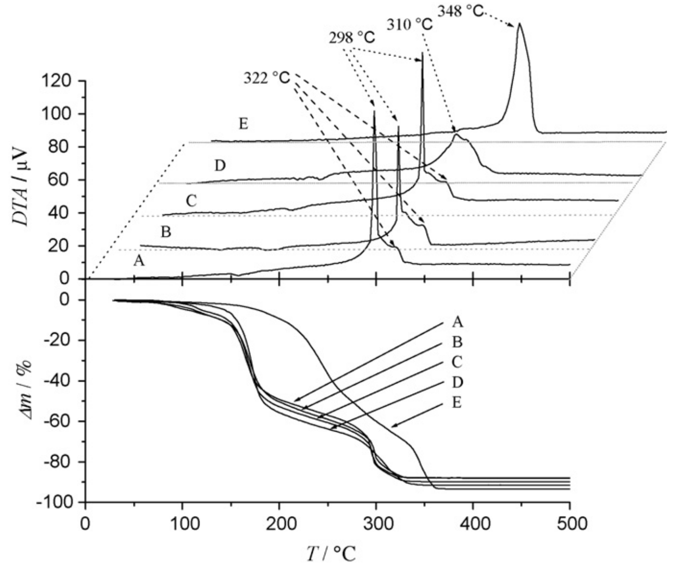

Fig. 2. TG–DTA plots of gels in air.

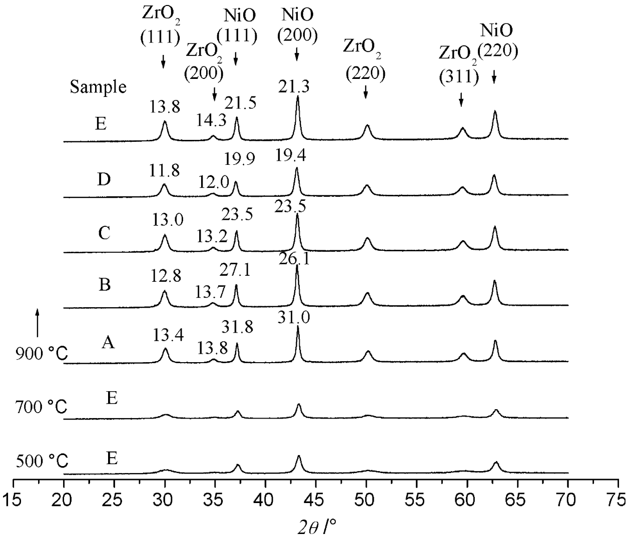

Fig. 3. X-ray diffraction patterns of powders calcined at 500 °C, 700 °C and 900 °C for 1 h and their calculated crystallite size (values are presented in nm).

3. Results and discussion

Thermal analysis was used in order to determine the thermal effects and mass losses that occurred during the heat treatment of the reactive gels (Fig. 2). For all samples the weight loss occurred in several steps and increased on increasing the amount of CA and EG in the starting solution from 87.7% for sample A to 93.3% for sample E. The results show that an increase of CA in the starting solution resulted in the decomposition of samples at slightly higher temperatures. The decomposition of sample A, prepared with CA/EG = 1.5, thus started at 75 °C and ended at 340 °C, while sample D, prepared with CA/EG = 5, started to decompose at 110 °C and ended at 364 °C. In the case of sample E these two temperatures shifted to 130 °C and 382 °C, respectively. Because the CA/M ratio for samples D and E was the same, we attributed the relatively high decomposition temperature interval in the case of sample E to the change which had occurred during synthesis, e.g. the change of reaction medium from an aqueous to an organic one, and the consequent rise in the solution temperature.

The DTA plots of all samples showed a weak endothermic region in the temperature interval from 100 °C to 200 °C, which agrees with the data presented in the paper of Laberty-Robert et al. [5]. The authors attributed this region to the superposition of two reactions: dehydration of the reactive gel and evaporation of excess EG. This endothermic region was followed by another rather distinctive exothermic one for which the path of the curves and the areas under the peaks were similar for samples A–C. For samples D and E this DTA peak temperature was shifted from 310 °C to 348 °C, respectively. At the same time the peak area increased with increasing amount of organic material in the gels. According to Fig. 2 the exothermic peak in the temperature region from 250 °C to 350 °C was a consequence of at least two consecutive effects. The first exothermic effect at 298 °C for samples A–C was more pronounced if the total amount of organic additives (CA and EG) remained relatively low. With increase in the amount of CA and EG added to the precursor preparation, the second endothermic effect slowly prevailed (310 °C and 348 °C for samples D and E, respectively).

X-ray diffraction patterns of the powders made from dried gels are shown in Fig. 3. For presentation of the crystallinity of the samples two diffraction patterns at 500 °C and 700 °C are shown. All samples prepared at 500 °C exhibited the presence of NiO and ZrO_2 with cubic structure. On increasing the temperature of the thermal treatment a higher degree of crystallinity was obtained. By variation of CA/EG and EG/M ratios samples with various crystallite sizes could be prepared. The crystallite sizes in samples calcined at 900 °C for 1 h were determined by the use of the Scherrer equation and are presented in Fig. 3. For samples A–D the crystallite size of both constituents was reduced, presumably due to the increasing amount of CA in the starting solution. The reduction of crystallite size was approximately 12% for ZrO_2-cubic and 37% for NiO compared to the initial value of sample A. With the shift from aqueous (sample D) to organic media (sample E), the crystallite size of both ZrO_2-cubic and NiO constituents increased, e.g. around 15% for ZrO_2-cubic and around 8% for NiO. The crystallite sizes of 14.3 nm for ZrO_2-cubic in sample E and of 31.8 nm for NiO in sample A represented the highest values obtained of all the samples. In general an increase in the amount of citric acid reduced ZrO_2 and NiO crystallite sizes, whereas the shift from aqueous to organic media had the opposite effect, e.g. the crystallite sizes of constituents were increased.

The specific surface area of powder samples calcined at 900 °C for 1 h was determined by the one point BET method. The results for sample A–E were (10.1 ± 0.1); (13.8 ± 0.1); (15.8 ± 0.1); (15.4 ± 0.2) and $(27.4 \pm 0.2)\ m^2\ g^{-1}$, respectively. The specific surface area of samples A–C increased with the increasing amount of citric acid in the starting solution. If the deviation of the measurements is taken into consideration, one can conclude that higher additions of CA (samples C and D) had a minimal effect on the specific surface value. However, on increasing the amount of EG in the starting solution the specific surface area of the products (sample E) could be substantially raised. According to the literature data the thermal decomposition of organo-metallic complexes to metallic oxides precedes through the formation of corresponding metal carbonates [9]. A larger amount of carboxylic complexes in the starting solution, i.e. samples A–C, leads to an increase of CO_2 evolution during the thermal decomposition and to higher specific surface values in the powders produced. The specific surface value of sample D did not further increase compared to sample C because further increase of the CA/M ratio had a minimal effect on the chemical structure of the precursors. The additional increase of specific surface area in sample E originates from an increase in the degree of polymerisation between CA and EG in the resin [9].

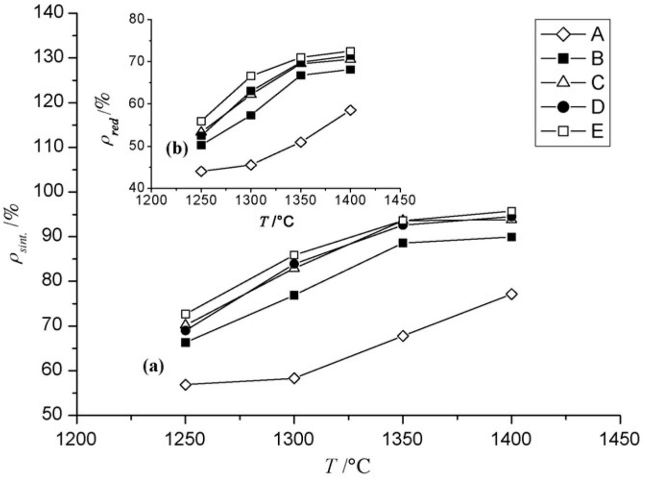

Fig. 4. Temperature dependence of relative sintering density (a) and relative reduced density (b) of different samples.

The sinterability of NiO–YSZ powders is shown in Fig. 4a as the relative sintered density at designated temperatures. Prior to sintering at different temperatures for 1 h the pellets relative green densities were adjusted to 42.2 ± 0.2% of the theoretical value of 6.488 g cm^{-3}. In the temperature interval from 1250 °C to 1400 °C the sintered densities of the samples increased by around 24%. At 1400 °C samples A–E reached values of 77.2%, 89.9%, 93.8%, 94.5% and 95.7% of the theoretical density, respectively. These results show the poor sinterability of sample A compared to the other samples, which could be attributed to the presence of hard agglomerates in the calcined powder. This assumption was later confirmed by SEM analysis. On the other hand, samples B–E exhibited generally similar sintering behaviour, i.e. the main increase in densification occurred in the temperature region from 1250 °C to 1350 °C. However, the relative sintered densities of sample E were the highest in the whole interval and reached values of 85.6% and 93.6% when sintered at 1300 °C or 1350 °C, respectively. Such relatively high values suggest that both phases (NiO and YSZ) form continuous paths through the whole sample.

The observed sintering characteristics of the pelleted samples were in accordance with the BET measurements of the corresponding powders. In general, higher measured BET values of powders result in lower sintering temperatures and higher sintered densities. Since the two phases (NiO and YSZ) sinter separately, relatively low sintering temperatures are essential if SOFC anode elements are prepared from such mixtures. If the sintering temperature can be kept in the region around 1300 °C or lower, one phase dominance after the final thermal treatment remains in the sub-micron region.

The sintered pellets were subsequently subjected to heat treatment (2 h at 900 °C) in an Ar ($\varphi = 0.95$)–H_2 ($\varphi = 0.05$)

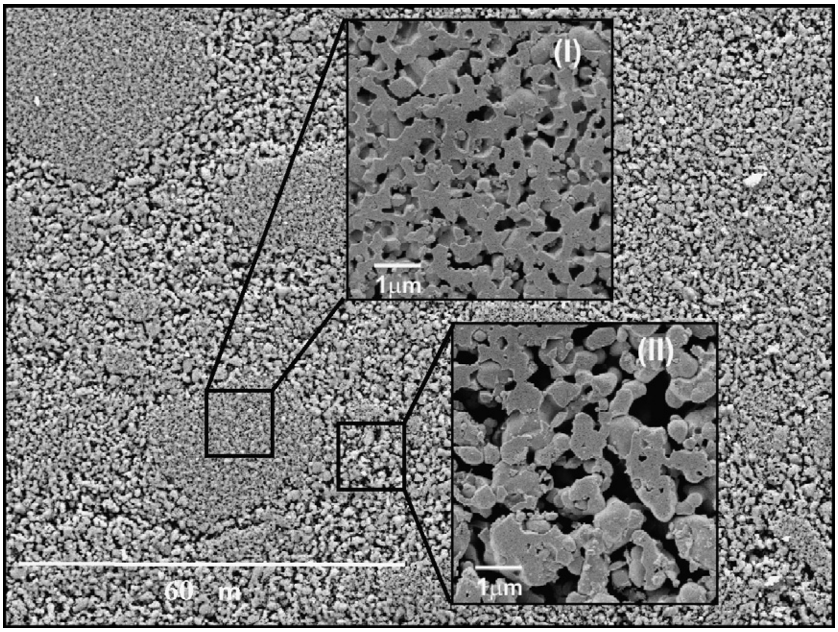

Fig. 5. Photomicrographs of sample A sintered at 1300 °C and subsequently reduced.

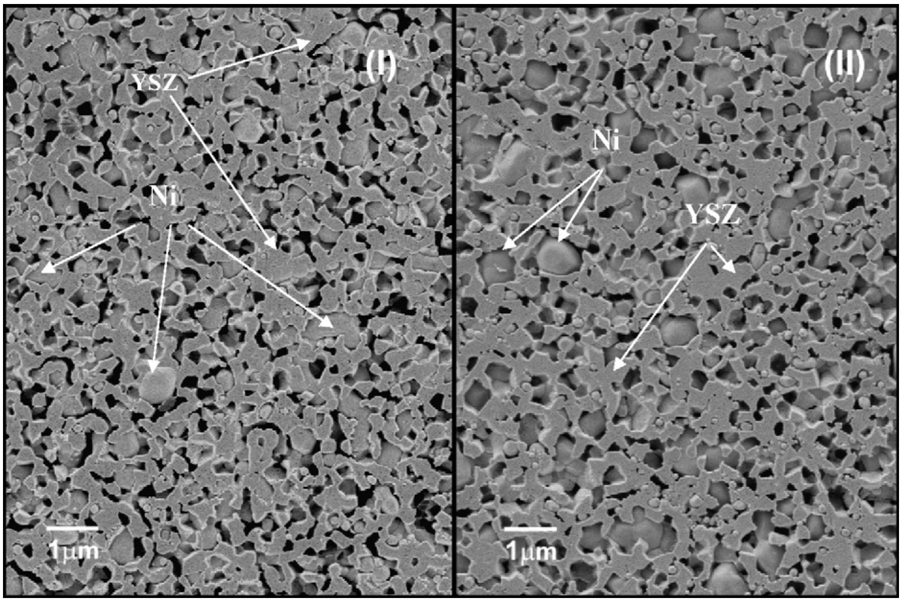

Fig. 6. Photomicrographs of samples B (I) and D (II) sintered at 1300 °C and subsequently reduced.

atmosphere to reduce NiO to Ni. The relative reduced densities of pellets were calculated from their geometrical densities relative to the theoretical density of Ni–YSZ cermet (7.436 g cm^{-3}). The change of the relative reduced density with temperature is presented in Fig. 4b. We observed that during reduction the dimensions of the pellets did not change. This fact indicated that the ceramic matrix retained the structure which formed during sintering. The property is important because a stable ceramic matrix retains the dispersion of nickel particles and the porosity of the cermet material during potential long-term operations of fuel cells [2].

The microstructure of samples sintered at various temperatures and the distribution of Ni and YSZ constituents throughout the composites are presented in Figs. 5–7. The microstructures in Fig. 5 represent sample A sintered at 1300 °C and subsequently reduced. These microstructures confirm the poor sinterability of sample A in comparison with the much more homogeneous microstructures of the other samples. Sample A is composed of larger agglomerates in which the microstructure seems denser (Fig. 5I) compared to the surrounding area (Fig. 5II). Energy-dispersive X-ray analysis (EDS) (not presented in this article) showed that all segments in sample A are composed of relatively large (around 1 μm) regions of one phase dominance. Such a microstructure implies that due to an insufficient amount of CA present in the precursor reaction mixture, there was inadequate reactive gel

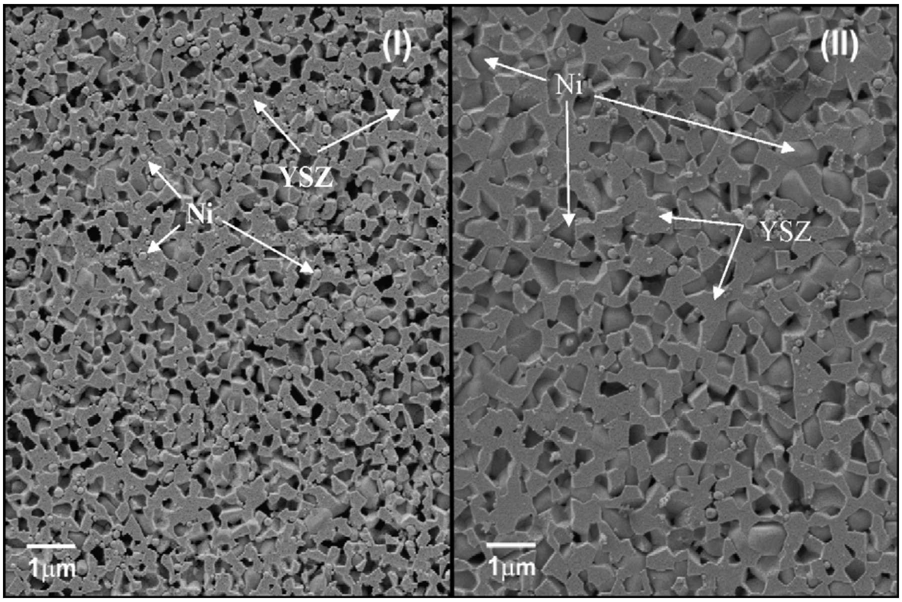

Fig. 7. Photomicrographs of sample E sintered at 1300 °C (I) and 1400 °C (II) and subsequently reduced.

formation. On doubling the amount of CA in the starting solution the regions of one phase dominance in the final product were reduced (sample B, Fig. 6I). The final microstructure was not significantly altered when even higher CA/EG initial ratios (sample D, Fig. 6II) were used. The most homogeneous distribution of the two phases was obtained in sample E (CA/EG = 0.2, EG/M = 25) prepared with the highest initial addition of EG. The size of Ni grains ranged from 0.10 μm to 0.23 μm. Comparison of the microstructure of sample E sintered at 1300 °C (Fig. 7I) and 1400 °C (Fig. 7II) revealed that the major part of the densification and phase distribution processes are completed up to 1300 °C. Further sintering above this temperature causes an undesired phase overgrowth, without substantial change in the sample density but accompanied by a rather high reduction of triple-phase boundaries.

4. Conclusions

The polymerised complex method was successfully used for the preparation of Ni–YSZ anode material where change in the CA/EG molar ratio ranging from 5 to 0.2 and various sintering temperatures were investigated in order to determine the correlation between synthesis parameters and the final characteristics of the Ni–YSZ anode material. The thermal behaviour of the gels, studied by the thermal analysis, is influenced to a large extent by the CA/EG and CA/M ratios. An increase of CA and EG in the starting solution increased the final temperature of thermal decomposition of the gels (from 340 °C to 382 °C) and consequently the specific surface area of the calcined NiO–YSZ powders. The specific surface area of NiO–YSZ powders decreased with increase in the CA/EG molar ratio from $(27.4 \pm 0.2)\ \mathrm{m^2\ g^{-1}}$ for sample E to $(10.1 \pm 0.1)\ \mathrm{m^2\ g^{-1}}$ for sample A. XRD analysis revealed that NiO and ZrO_2 crystalline phases first formed in samples calcined at 500 °C. The crystallite size of the different phases depends on the CA/EG ratio. By increasing the amount of citric acid the crystallite size of NiO and YSZ decreased (samples A–D) for samples calcined at 900 °C. When the reaction media changed from an aqueous to an organic one (sample E), an opposite effect was observed for both constituents.

The effect of different annealing temperatures on the sintered and reduced density and microstructure of the pellets obtained was examined. The results showed that by increasing the amount of CA and EG in the starting solution the relative sintered and reduced densities of the samples increased by around 24% in the temperature range from 1250 °C to 1400 °C. The sample with the highest addition of EG (sample E) exhibited the highest sinterability compared to the other samples. The relative sintered density, obtained after annealing the sample for 1 h at 1300 °C and relative reduced density, obtained after consequent reduction, were 85.9% and 66.6% of the theoretical density, respectively. SEM analysis combined with the results from sintering studies showed that samples sintered above 1300 °C exhibited in parallel to densification, growth of NiO and YSZ grains. The Sample with a ratio CA/EG = 5/25 (sample E) had the most homogeneous microstructure and the smallest Ni grains (around 0.2 μm) compared to other samples. This effect was attributed to the change from an aqueous to an organic medium during the synthesis and to the consequent rise of the solution temperature.

Acknowledgement

This research was supported by the Ministry of Higher Education, Science and Technology of Republic of Slovenia (3311-02-831718).

References

[1] C. Song, Fuel processing for low-temperature and high-temperature fuel cells: challenges, and opportunities for sustainable development in the 21st century, Catal. Today 77 (1–2) (2002) 17–49.

[2] C. Subhash, K. Singhal, Kendall, High Temperature Solid Oxide Fuel Cells: Fundamentals Design and Applications, Elsevier Corp., Oxford, New York, Tokyo, 2003.

[3] L.E. Smart, E.A. Moore, Solid State Chemistry: An Introduction, 3rd Ed., CRC Press, Boca Raton [FL], Taylor & Francis, 2005.

[4] M.P. Pechini, Method of preparing lead and alkaline earth titanates and niobates and coating method using the same to form a capacitor, US Patent No. 3,330,697 1967.

[5] Ch. Laberty-Robert, F. Ansart, C. Deloget, M. Gaudon, A. Rousset, Powder synthesis of nanocrystalline ZrO_2–8%Y_2O_3 via a polymerization route, Mater. Res. Bull. 36 (2001) 2083–2101.

[6] Ch. Laberty-Robert, F. Ansart, C. Deloget, M. Gaudon, A. Rousset, Dense yttria stabilized zirconia: sintering and microstructure, Ceram. Int. 29 (2003) 151–158.

[7] P. Durán, J. Tartaj, F. Capel, C. Moure, Processing and characterisation of a fine nickel oxide/zirconia/composite prepared by polymeric complex solution synthesis, J. Eur. Ceram. Soc. 23 (2003) 2125–2133.

[8] S.-D. Kim, H. Moon, S.-h. Hyun, J. Moon, J. Kim, H.-W Lee, Performance and durability of Ni-coated YSZ anodes for intermediate temperature solid oxide fuel cells, Solid State Ion 177 (2006) 931–938.

[9] W.-D. Yanga, Y.-H. Changb, S.-H. Huangb, Influence of molar ratio of citric acid to metal ions on preparation of $La_{0.67}Sr_{0.33}MnO_3$ materials via polymerizable complex process, J. Eur. Ceram. Soc. 25 (2005) 3611–3618.

[10] C. Hammond, The Basics of Crystallography and Diffraction, 2nd Ed., Oxford university press, Oxford, 2001.